

A 3D Two-node and One-node HCMFD Algorithm for Pin-wise Reactor Analysis

Jaeha Kim and Yonghee Kim

Korea Advanced Institute of Science and Technology (KAIST)

291 Daehak-ro, Yuseong-gu, Daejeon, Korea, 34141

*Corresponding author: yongheekim@kaist.ac.kr

1. Introduction

Conventionally, the pin-power reconstruction method in conjunction with an assembly-wise nodal analysis has been a standard way to obtain a pin-level solution since a pin-wise analysis is costly and time-consuming. If one can overcome these limitations, a pin-wise reactor analysis is expected to be one nice way to obtain a detailed pin-level solution. Recently, the HCMFD (Hybrid Coarse-Mesh Finite Difference) algorithm has been suggested as a breakthrough for the pin-wise approach by which parallel computing can be performed very effectively [1-3].

To maximize parallel computational efficiency, an iterative local-global strategy is adopted in the HCMFD algorithm. The global eigenvalue problem is solved by one-node CMFD, and the local fixed-source problems are solved by two-node CMFD based on the pin-wise nodal solutions. In such a local-global scheme, the computational cost is mostly concentrated in solving local problems which can be solved in parallel, enabling the effective application of parallel computing.

Previously, the feasibility of the HCMFD algorithm was evaluated only in a 2-D scheme. In this paper, the 3D HCMFD algorithm with some possible variations in treating the axial direction is introduced.

2. Methodology

In the HCMFD algorithm, two CMFD methods are nonlinearly coupled for the iterative local-global strategy, as shown in Fig. 1. The solution of the global eigenvalue problem provides the basis for the local fixed-source problems, and the solutions of the local problems are used as reference quantities to produce the correction factors for the global one-node CMFD.

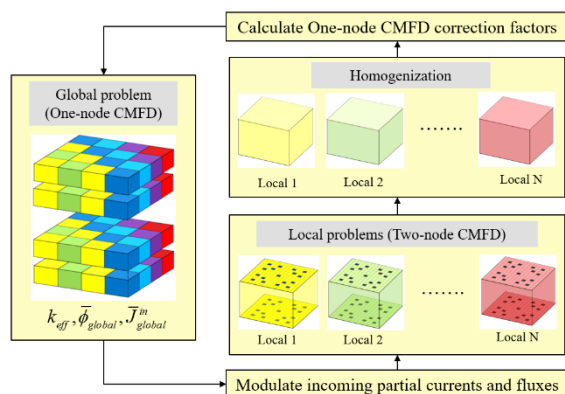


Fig. 1. Schematic diagram of HCMFD algorithm

In the x - y plane, each single fuel assembly was treated as a coarse mesh in the one-node CMFD, while the pin-wise mesh is actually considered for the higher-order solution. Unlike the 2-D case, the axial (z -directional) node size in local problems can be much bigger than that in the x - y directions and the aspect ratio of the 3D node can be very far from unity in 3-D applications of the HCMFD algorithm.

As in the 2D scheme, the standard NEM (nodal expansion method) based on the 4th-order polynomials is used in pin-level for the x - y directions. Meanwhile, for the axial direction, several variations are given on the axial mesh size and even on the method itself in this work.

When there exists a non-negligible heterogeneity in the axial direction, the axial direction should also be treated sufficiently accurately and one easy way is to divide the axial coarse mesh into several meshes. However, since the more mesh divisions in the axial direction also means an increase in the number of the radial interfaces by several times in a 3-D scheme, it would be desirable to achieve the desired axial accuracy with a minimum number of mesh divisions. For this, the ANM (Analytic Nodal Method) is also tried in this paper only for the axial nodal analysis as in Fig. 2, by which one can get a better solution with the same mesh size but with more cost than by the NEM.

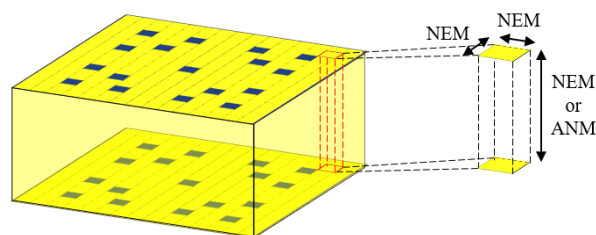


Fig. 2. Nodal methods used in each direction

2.1 One-node CMFD for Global Eigenvalue Problem

As in Fig. 3, two correction factors are introduced for each interface in the one-node CMFD method. The two correction factors are produced as Eq. (1) and (2) using the reference surface flux and net current, and they are implemented in the global net current formulation as Eq. (3) to preserve the reference higher-order surface-average information. In this case, the reference surface-averaged flux and net current are calculated by taking the average of the quantities obtained from local fine-mesh nodal calculations.

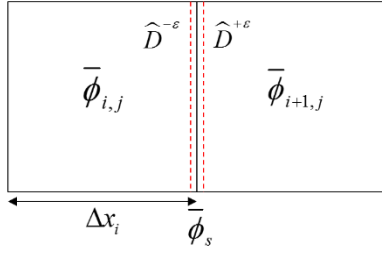


Fig. 3. Inner interface in one-node CMFD

$$\hat{D}^{-\varepsilon} = -\frac{\Delta x \cdot \bar{J}_s^{ref} + 2D_i(\bar{\phi}_s^{ref} - \bar{\phi}_i)}{2(\bar{\phi}_s^{ref} + \bar{\phi}_i)} \quad (1)$$

$$\hat{D}^{+\varepsilon} = -\frac{\Delta x \cdot \bar{J}_s^{ref} + 2D_{i+1}(\bar{\phi}_{i+1} - \bar{\phi}_s^{ref})}{2(\bar{\phi}_s^{ref} + \bar{\phi}_{i+1})} \quad (2)$$

$$\bar{J}_s = \frac{2(D_i - \hat{D}^{-\varepsilon})(D_{i+1} - \hat{D}^{+\varepsilon})}{\Delta x(D_i + D_{i+1} + \hat{D}^{-\varepsilon} - \hat{D}^{+\varepsilon})} \bar{\phi}_i - \frac{2(D_i + \hat{D}^{-\varepsilon})(D_{i+1} + \hat{D}^{+\varepsilon})}{\Delta x(D_i + D_{i+1} + \hat{D}^{-\varepsilon} - \hat{D}^{+\varepsilon})} \bar{\phi}_{i+1} \quad (3)$$

2.2 Two-Node CMFD for Local Fixed-Source Problem

In the two-node CMFD approach, only one correction factor is introduced for each interface as described in Fig. 4 to preserve the net current. The correction factor is determined using reference net currents as Eq. (4) and (5) and it is used in the net current formulation as Eq. (6) to preserve the reference net current. In the current nodal-based HCMFD, the reference net current is obtained by pin-wise NEM or ANM calculation.

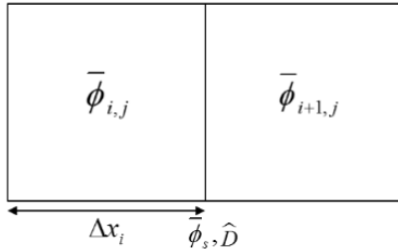


Fig. 4. Inner interface in one-node CMFD

$$\hat{D}_{ii+1} = \frac{-\tilde{D}_{ii+1}(\bar{\phi}_{i+1} - \bar{\phi}_i) - \bar{J}_{ii+1}^{ref}}{(\bar{\phi}_{i+1} + \bar{\phi}_i)} \quad (4)$$

$$\tilde{D}_{ii+1} = 2 \frac{D_i}{\Delta x_i} \frac{D_{i+1}}{\Delta x_{i+1}} / \left(\frac{D_i}{\Delta x_i} + \frac{D_{i+1}}{\Delta x_{i+1}} \right) \quad (5)$$

$$\bar{J}_{ii+1} = -\tilde{D}_{ii+1}(\bar{\phi}_{i+1} - \bar{\phi}_i) - \hat{D}_{ii+1}(\bar{\phi}_{i+1} + \bar{\phi}_i) \quad (6)$$

Since the local problems are fixed-source problems, the incoming partial currents are given on the boundary. The correction factor and corrected net current on the boundary, especially for the right-end boundary, are expressed as Eqs. (7) and (8). Those for the left-end boundary can similarly be obtained. In 3-D HCMFD, this process is repeated for all 3 directions.

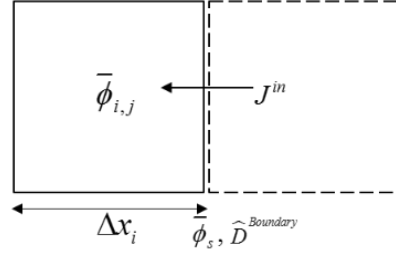


Fig. 5. Right-end boundary in two-node CMFD

$$\hat{D}_{i,right} = \frac{2D_i\bar{\phi}_i - (\Delta x_i + 4D_i)\bar{J}_s^{ref} - 8D_i\bar{J}^-}{2\bar{\phi}_i + 4\bar{J}_s^{ref} + 8\bar{J}^-} \quad (7)$$

$$\bar{J}_{s,right} = \frac{2(D_i - \hat{D}_i)}{\Delta x_i + 4(D_i + \hat{D}_i)} \bar{\phi}_i + \frac{-8(D_i + \hat{D}_i)}{\Delta x_i + 4(D_i + \hat{D}_i)} \bar{J}^- \quad (8)$$

Basically, the global node balance is implemented to each local problem in terms of the modulated fluxes, and the boundary conditions are given by the modulated incoming partial currents. For a better convergence, the local two-node CMFD calculation is performed twice per one local analysis, with an overall exchange of partial currents and transverse leakages between local problems. In this way, the newest high-order quantities evaluated by solving a local problem can be reflected in neighboring local problems in real time, so that the convergence can be accelerated and also the possible numerical instability at the early stage of the local-global iteration can be eliminated.

3. Numerical Results

In this work, a 2-D modified EPRI-9R benchmark problem described in Fig. 6 was simply extended to a 3-D problem as in Fig. 7. The active core height is set to be 200cm with upper and lower 20cm reflector layers, and the coarse mesh height is 20cm. In this study, two cases were considered to see the sensitivity regarding the axial partitioning, one with the central control rod fully inserted (Case 1), and the other case with the control rod inserted to the mid-plane of the active core (Case 2).

The convergence criterion for the fission source and eigenvalue was 10^{-7} , and the local and global problems were both solved by a BiCGSTAB (Biconjugate gradient stabilized) method [4]. The local analysis was performed every 10 global outer iterations, which is an optimized number in terms of computing time for the two 3-D cases. All calculations were performed on Intel Xeon E5-2697 v3 2.60 GHz CPU. Parallel computation was performed using the OpenMP parallel algorithm [5] in this study.

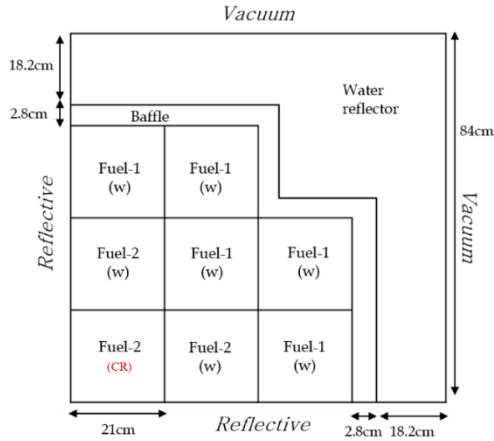


Fig. 6. 2-D modified EPRI-9R benchmark problem

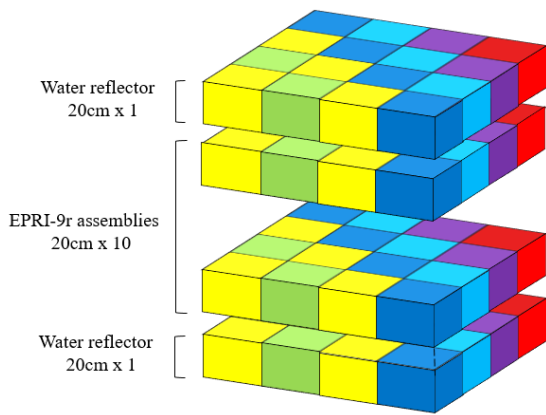


Fig. 7. 3-D extension of EPRI-9R benchmark problem

First, the parallelizable portion of the whole computational loads, the so-called parallelism, depending on the axial partition was briefly analyzed in Case 1 with NEM for the axial direction (Table I). Even with the minimum axial partition with a 20 cm mesh size, the parallelism is 99.48%, and it further increases to 99.98% when the number of axial nodes is increased by a factor of 10. Table I indicates that the parallel computational efficiency of the 3D HCMFD algorithm can possibly be quite high.

Table I: Parallelism in Case 1

Method	Mesh size (cm)	Parallelism (%)
HCMFD-NEM	$1.4 \times 1.4 \times 20$	99.48
HCMFD-NEM	$1.4 \times 1.4 \times 2$	99.98

With the OpenMP parallel architecture, the parallel computational efficiency was analyzed in Case 1 with two different axial partitions and the results are shown in Table II. As expected, the overall parallel computational efficiency is better in the cases with more axial divisions and the parallel efficiency for 20 cores is 50~59% for a relatively small size problem.

Table II: Parallel Computational Efficiency in Case 1

No. of core	Axial layers per local problem	CPU time (sec)	Speed-up	Efficiency (%)
1	1	22.04	-	--
2	1	11.44	1.93	96.33
5	1	5.66	3.89	77.88
10	1	3.37	6.54	65.40
20	1	2.16	10.20	51.02
1	4	144.89	-	--
2	4	75.00	1.93	96.59
5	4	36.68	3.95	79.00
10	4	20.88	6.94	69.39
20	4	12.38	11.70	58.52

To investigate the numerical performances depending on the number of axial layers and the type of nodal method in local problems, two benchmarks were solved by NEM and ANM with various axial partitions as shown in Table III and IV. For comparison, fine-mesh FDM solutions are also included, but it should be noted that they cannot be true references since the mesh size for FDM was not small enough. In this work, the k_{eff} values by HCMFD with 10 axial layers were chosen as reference values.

In Table III, one can note that the axial mesh refinement results in a converged solution for the two cases. For the 1st benchmark (Case 1), both of the axial NEM and ANM with a coarse mesh (10~20cm) can provide accurate solutions, while the solution is more sensitive to the axial mesh size in Case 2. This is because the axial flux profile is rather smooth in Case 1 and it is strongly position-dependent due to the partial insertion of the control rod.

In case of high axial heterogeneity, the axial mesh size for the NEM should be rather small, 5~10cm, for a reasonably accurate solution. When the ANM is used for the axial direction in Case 2, the k_{eff} error is smaller than that by NEM with an axial mesh size smaller than 10cm. However, the improvement in accuracy is not satisfactory when compared to the conventional tendency between NEM and ANM. It is supposed that it to be due to that It seems that some more improvement is required to adapt the ANM in HCMFD algorithm.

Table III: Sensitivity in k_{eff} , Case 1

Method	Mesh size	k_{eff}	Error (pcm)
FDM	$0.2 \times 0.2 \times 2$	0.881083	1.2
HCMFD-NEM	$1.4 \times 1.4 \times 2$	0.881071	Ref.
HCMFD-NEM	$1.4 \times 1.4 \times 20$	0.881047	2.4
HCMFD-NEM	$1.4 \times 1.4 \times 10$	0.881069	0.2
HCMFD-NEM	$1.4 \times 1.4 \times 5$	0.881071	0.0
HCMFD-ANM	$1.4 \times 1.4 \times 20$	0.881077	0.5
HCMFD-ANM	$1.4 \times 1.4 \times 10$	0.881073	0.2
HCMFD-ANM	$1.4 \times 1.4 \times 5$	0.881071	0.0

Table IV: Sensitivity in k-eff, Case 2

Method	Mesh size (cm)	k_{eff}	Error (pcm)
FDM	0.2×0.2×1	0.905650	-5.0
HCMFD-NEM	1.4×1.4×2	0.905700	Ref.
HCMFD-NEM	1.4×1.4×20	0.905876	17.6
HCMFD-NEM	1.4×1.4×10	0.905755	5.5
HCMFD-NEM	1.4×1.4×5	0.905712	1.2
HCMFD-ANM	1.4×1.4×20	0.905883	18.3
HCMFD-ANM	1.4×1.4×10	0.905746	4.6
HCMFD-ANM	1.4×1.4×5	0.905709	0.9

4. Conclusions

The HCMFD algorithm was successfully extended to a 3-D core analysis without any numerical instability even though the axial mesh size in local problems is quite different from the x - y node size. We have shown that 3D pin-wise core analysis can be done very effectively with the HCMFD framework. Additionally, it was demonstrated that parallel efficiency of the new 3D HCMFD scheme can be quite high on a simple OpenMP parallel architecture. It is concluded that the 3D HCMFD will enable an efficient pin-wise 3D core analysis.

REFERENCES

- [1] Seongho Song, Hwanyael Yu, and Yonghee Kim, "An Efficient One-Node and Two-Node Hybrid CMFD method," *Proceedings of the Korean Nuclear Society Autumn Meeting*, Gyeongju, South Korea, October 29-30, 2015.
- [2] Seongho Song, Hwanyael Yu, and Yonghee Kim, "Pin-by-Pin Reactor Core Analysis Based on a NEM-based Two-level Hybrid CMFD Algorithm," *Proceedings of PHYSOR 2016*, Sun Valley, Idaho, USA, May 1-5, 2016.
- [3] Seongho Song, Hwanyael Yu, and Yonghee Kim, "Pin-by-Pin Core Calculation with an NEM-Based Two-Level Hybrid CMFD Algorithm," *Transactions of ANS 2016*, New Orleans, USA, June 12-16, 2016.
- [4] H.A. Van Der Vorst, "Bi-CGSTAB: A Fast and Smoothly Converging Variant of Bi-CG for the Solution of Nonsymmetric Linear Systems", *SIAM J. Sci. and Stat. Comput.*, 13(2), 631–644, 1991.
- [5] OpenMP API, "OpenMP Application Program Interface", Version 4.0, July, 2013.